Hindawi Publishing Corporation
Journal of Nanotechnology
Volume 2012, Article ID 709031, 6 pages
doi:10.1155/2012/709031

Research Article

Interconnected TiO_2 Nanowire Networks for PbS Quantum Dot Solar Cell Applications

Fan Xu,[1] Jaime Benavides,[1] Xin Ma,[1] and Sylvain G. Cloutier[1,2]

[1] *Department of Electrical and Computer Engineering, University of Delaware, 140 Evans Hall, Newark, DE 19716, USA*
[2] *Département de Génie Électrique, École de Technologie Supérieure, 1100 rue Notre-Dame Ouest, Montréal, QC, Canada H3C1K3*

Correspondence should be addressed to Sylvain G. Cloutier, sylvaing.cloutier@etsmtl.ca

Received 21 November 2011; Revised 7 February 2012; Accepted 15 February 2012

Academic Editor: Sharad D. Bhagat

We present a simple method for the fabrication of an interconnected porous TiO_2 nanostructured film via dip coating in a colloidal suspension of ultrathin TiO_2 nanowires followed by high-temperature annealing. The spheroidization of the nanowires and the fusing of the loosely packed nanowire films at the contact points lead to the formation of nanopores. Using this interconnected TiO_2 nanowire network for electron transport, a PbS/TiO_2 heterojunction solar cell with a large short-circuit current of 2.5 mA/cm^2, a Voc of 0.6 V, and a power conversion efficiency of 5.4% is achieved under 8.5 mW/cm^2 white light illumination. Compared to conventional planar TiO_2 film structures, these results suggest superior electron transport properties while still providing the large interfacial area between PbS quantum dots and TiO_2 required for efficient exciton dissociation.

1. Introduction

Lead chalcogenide colloidal semiconductor nanocrystals can be promising materials for low-cost, large-area, and efficient photovoltaic devices, due to a large Bohr radius, size-effect tunable bandgap across the near-infrared region and large absorption cross-section, as well as the solution processability [1–7]. Over the last few years, Schottky solar cells based on PbS, PbSe, or PbS_xSe_{1-x} quantum dots with power converting efficiency over 3% have been demonstrated [3, 5, 7]. More recently, the depleted-heterojunction quantum dots solar cells based on the PbS/TiO_2 nanocrystals have achieved an unprecedented efficiency of 5.1% [1], and PbS/ZnO photovoltaic devices have exhibited excellent air stability for 1000 h of continuous illumination under ambient atmosphere [2].

In general, the power conversion efficiency of the QDs solar cells is primarily determined by three factors: exciton generation, exciton dissociation, and carrier collection efficiencies. Indeed, it was shown previously that the structure and morphology of the TiO_2 layer can play the key role in achieving efficient extraction and transport of minority carriers in dye- and QDs-sensitized solar cells [8]. The TiO_2 layer requires large surface areas for quantum dots attaching, as well as rapid electron transport across the film to ensure efficient electron collection by the conductive substrate. The widely used mesoporous TiO_2 nanostructured films can be employed to significantly increase the contact area between TiO_2 and the active quantum dot layer, thus facilitating exciton dissociation before radiative recombination and allowing efficient carrier collection. However, the electronic transport suffers from slow electron diffusion rates and low electron mobility in the structurally disordered TiO_2 mesoporous films [8, 9].

Fabrication of TiO_2 films from one-dimensional nanowire and nanotube structures has proven to be an effective way to improve the overall efficiencies of the devices [9–12]. The one-dimensional nanostructure allows diffusion free electron transport along the axial direction to improve electron collection, while the light scattering effect from the subwavelength features can enhance the effective absorption thickness of the quantum dots layer. Nevertheless, one major concern with lateral nanowires is the smaller surface areas it presents for dye and quantum dot sensitization [8].

In this paper, we report the fabrication of superior TiO_2 film structures for QD solar cells formed by dip coating and annealing of ultrathin TiO_2 nanowire films. This interconnected nanowire network structure maintains the large

surface-to-volume ratio from traditional porous TiO_2 films, while allowing efficient electron transport along the nanowires. As we show, the electron transport and carrier extraction in the TiO_2/PbS heterojunction solar cell can be significantly improved using this porous interconnected TiO_2 nanowire network film. A superb low-cost solar cell was fabricated with a large short-circuit current of 2.5 mA/cm^2, a V_{oc} of 0.6 V, and a power conversion efficiency of 5.4% achieved under 8.5 mW/cm^2 illumination.

2. Experiments

2.1. Chemicals. Titanium (IV) butoxide 99% (TBT, Aldrich), oleic acid (90%, Aldrich), titanium (IV) isopropoxide (TTIP, Aldrich, 99.999%), poly(acrylic acid) (M 450,000, Aldrich), ethyl acetate (Aldrich, Anhydrous 99.8%) (EAcAc), ethanol (ACS reagent, ≥99.5% (200 proof, absolute), 1-octadecene (90%, Aldrich), lead oxide (99.99%, Aldrich), hexamethyldisilathiane (Fluka) are used.

Preparation of TiO_2 Sol-Gel [13]. PAA (0.035 g) and EAcAc (1.7998 g) were mixed and sonicated at room temperature for 5 minutes. Ethyl alcohol (42.3429 g) was added and left reposed for 20 minutes. Finally, TBT (13.7489 g) was added to the mixture and was reposed for another 20 minutes, and distilled water (0.5457 g) was added to start the reaction. The solution was continuously stirred for 8 hours and then aged for 24 hours to form the TiO_2 sol-gel.

Synthesis of TiO_2 Nanowires [14]. The TiO_2 nanowires were synthesized through the nonhydrolytic ester elimination reaction of titanium isopropoxide and oleic acid. TTIP (3.5 mL) was added to 10 g of OA at room temperature under nitrogen atmosphere. The resulting mixture was heated to 280°C for a period of 20 min and was kept at this temperature for 2 h. The light-yellow solution gradually turned dark brown and then white. The solution was then cooled down to room temperature, excess acetone was added, and the solution was centrifuged to precipitate the nanowires.

PbS Quantum Dot Synthesis [15]. Lead oxide (0.45 g), octadecene (10 g), and oleic acid (1.34 g) are added to a three-neck flask. The mixture is then heated and kept at 80°C for two hours under vigorous stirring in vacuum to degas the solution and dissolve the mixture. Then, the temperature is kept at 110°C under nitrogen flow for 30 min. Subsequently, a solution made of 210 μL of hexamethyldisilathiane diluted in 4 mL of octadecene is quickly injected into the reaction flask under vigorously stirring. The heating was immediately removed and the reaction solution was allowed to cool down slowly to room temperature. Finally, the colloidal PbS quantum dots are collected by quick injection of the reaction solution into excess amount of acetone (with ratio ~1 : 4) for centrifugation. The precipitates are dried in vacuum and redispersed in hexane. To ensure adequate removal of the reaction solvents, precipitation and redispersion are repeated. The quantum dot solution is filtered with 0.2 μm polytetrafluoroethylene filters before device fabrication.

Fabrication of Solar Cells. The ITO glass was cleaned using a sequence of ultrasonic baths of deionized water, acetone and isopropanol. Then, the substrate was dipcoated into the TiO_2 sol-gel for 10 seconds and then withdrawn at 200 mm/min to form a thin layer of planar TiO_2 layer (~35 nm), in order to prevent any shorting of the device. This sol-gel TiO_2 layer was annealed at 500°C for 1 hour in a tube furnace to improve its crystalline structure and its conductivity. After that, the porous TiO_2 layers were fabricated by dip-coating the substrate (immersed in the nanowire solution for 10 seconds, and then withdrawn at 200 mm/min) into the TiO_2 nanowires solution in hexane (~35 mg/mL), followed by another annealing at 500°C for 1 hour in the furnace. To make the porous TiO_2 layer thicker, another layer of TiO_2 nanowire was dip-coated on top and then annealed. The PbS quantum dots are then deposited using the layer by layer spin-coating method [1]. For each cycle, the PbS quantum dot solution (25 mg/mL in hexane) is spin-coated (2000 rpm) on the substrate, then the diluted ethanedithiol solution in acetonitrile (0.02 M) is subsequently spin-coated on top to crosslink the quantum dot and make the quantum dot indissolvable in the original solution, and finally, hexane was spin-coated on the substrate to rinse the quantum dot solid [16]. For both devices, eight layers of quantum dots are deposited. Finally, gold is thermally evaporated on top as the back contact electrode. The solar cell was measured with devices placed on top of an integrated sphere under 8.5 mW/cm^2, white light illumination. The integrating sphere is connected to a fiber illuminator, and the light was uniformly coupled out from the top port of the integrate sphere.

3. Results and Discussions

As shown in Figure 1(a) the free-standing TiO_2 nanowires are typically 100–200 nm in length and 3-4 nm in diameter. As shown in Figure 1(b), the high-resolution TEM analysis of the TiO_2 nanowires confirms their sound crystalline structure. The FFT shown in the inset of Figure 1(b) indicates the nanowires are TiO_2 anatase, and it was imaged with its [100] direction parallel to the electron beam. Here, the long 18-carbon-atom stabilizing surfactant (oleic acid) plays a crucial role in passivating the nanowires to prevent agglomeration; thus a uniformly and loosely compacted TiO_2 nanowires film can be deposited by dip coating the substrate into the nanowire solution, as shown in Figure 2(a).

The TiO_2 nanowire fuse with each other at the contact point via sintering. On the other hand, the one-dimensional nanowire will reduce the aspect ratio and spheroidize owing to surface energy reduction [17]. When the spheroidization stops at the contact points of the nanowires, the porous structure is formed. Thus, a high-surface-area, interconnected porous TiO_2 nanostructure is fabricated using the facile dip-coating and annealing process, as shown in the SEM image in Figure 2(c). Large quantities of pores are distributed randomly on both the surface and the interior of the TiO_2 nanostructure. A high-resolution secondary electron SEM image in Figure 2(d) clearly resolved the porous structure of the film. The irregularly distributed nanopores

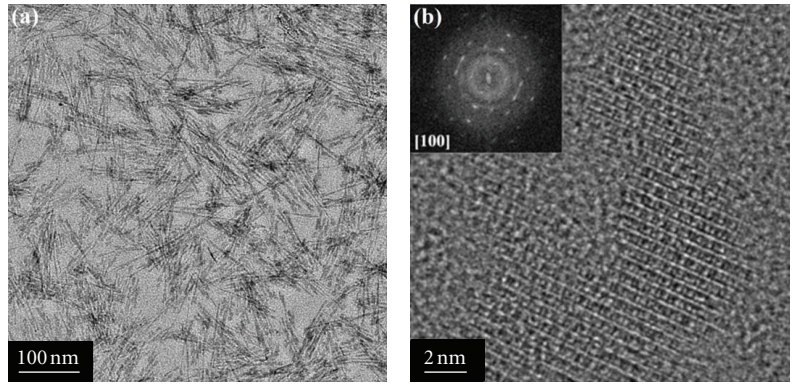

(a) (b)

Figure 1: (a) Low-resolution TEM image of the free-standing TiO_2 nanowires after synthesis. (b) The high-resolution TEM image of a single ultrathin TiO_2 nanowire, the inset shows the corresponding Fast Fourier Transform (FFT) image.

are interconnected by spheroidized NWs after thermal annealing process, with average diameter of 13.2 ± 4.7 nm and average pore area of $117 \pm 123\,nm^2$. Since the quantum dots used in these devices are typically 3-4 nm in diameter, the relatively larger nanopores can create additional volume for QDs attaching, as well as provide large surface areas to achieve efficient electron extraction.

The SEM image in Figure 3(a) shows the structure of the resulting solar cell device, while the band alignment is shown in Figure 3(b). All the fabrication steps except the evaporation are done in ambient atmosphere. The thickness of the planar TiO_2 is ~35 nm, the porous TiO_2 nanowire layer is ~60 nm, while the PbS quantum-layer is ~320 nm.

Figure 4 compares the current density-voltage (J-V) characteristics of a standard PbS quantum dot-sensitized TiO_2 heterojunction solar cell using a planar TiO_2 film formed by conventional sol-gel chemistry with the same solar cell using the thick nanoporous interconnected TiO_2 nanowire network previously deposited on a thin planar TiO_2 film. Here, small PbS quantum dots of relatively large bandgaps and with their conduction bands well above that of TiO_2 were used, so as to achieve efficient electronic transfer from the quantum dots to the TiO_2 [18]. For comparison, both the planar and porous TiO_2 heterojunction solar cells have equally thick PbS nanocrystalline layers and both were crosslinked using EDT. In contrast with the planar device, the TiO_2 nanowire device exhibits a superb short-circuit current (J_{sc}) of $2.5\,mA/cm^2$, a large open-circuit voltage (V_{oc}) of 0.6 V, a fill factor of 33%, and a power-converting efficiency of 5.4%. These results suggest that the large surface area in the porous TiO_2 nanostructured film, as well as an efficient carrier transport along the longitudinal axis of TiO_2 nanowires, appears to be critical to achieve high J_{sc} in the heterojunction solar cell architecture. The near-ideal rectifying J-V characteristics of the TiO_2 nanowire device under dark directly confirm the formation of a high-quality p-n heterojunction between PbS and TiO_2. In contrast, the planar TiO_2 solar cell device suffers from a much smaller short-circuit current (J_{sc}), in addition to a significantly lower fill factor of 14%. Moreover, the current drops down rapidly as the voltage starts to increase. Most likely, this can be attributed to the inefficient electron transport in the planar TiO_2 layer. Otherwise, it is also possible that pin holes are generated in the planar TiO_2 film during annealing, thus ruining the performance of the device and explaining the much larger currents observed under forward bias. Since the open-circuit voltage of the devices is mainly determined by difference of the quasi-Fermi level between the PbS nanocrystals and the TiO_2 layer, both devices exhibit a similar V_{oc} around 0.6 V.

To better understand the exciton dissociation and electron extraction from the PbS quantum dots to the TiO_2 we studied the absorption and photoluminescence of EDT-treated nanocrystalline films deposited on glass, planar TiO_2, and porous TiO_2 nanowire network films. Indeed, the electron transfer from small PbS nanocrystals to the TiO_2 can be monitored through the shift and quenching of the absorption and photoluminescence spectra [19, 20]. The conduction band of the small quantum dots lies well above that of the TiO_2 thus the high-energy excitons generated upon the absorption of high-energy photons in small QDs can rapidly dissociate with electrons injected to the TiO_2 layer. The porous TiO_2 nanowire structure provides large interfacial areas between QDs and TiO_2, thus enables efficient electron transfer [21]. This rapid relaxation of high-energy excitons can in turn improve the absorption of high-energy photon by rapid depopulating the excitons in the QDs. As seen in Figure 5(a), the absorption spectrum of the PbS nanocrystals deposited on porous TiO_2 nanowire structure displays a stronger absorption on the high-energy side and an obviously blue shift compared to the QDs deposited on planar TiO_2.

Meanwhile, the photoluminescence of the quantum dots is quenched owing to hot electron transfer to TiO_2. Figure 5(b) compares the photoluminescence of monolayer of nanocrystals deposited on glass, on planar TiO_2 and on the porous TiO_2, nanowire network. Due to the photoluminescence quenching at the high energy side, the photoluminescence of the PbS quantum dots exhibits a 24 nm red-shift on planar TiO_2, compared with a remarkable 76 nm red shift

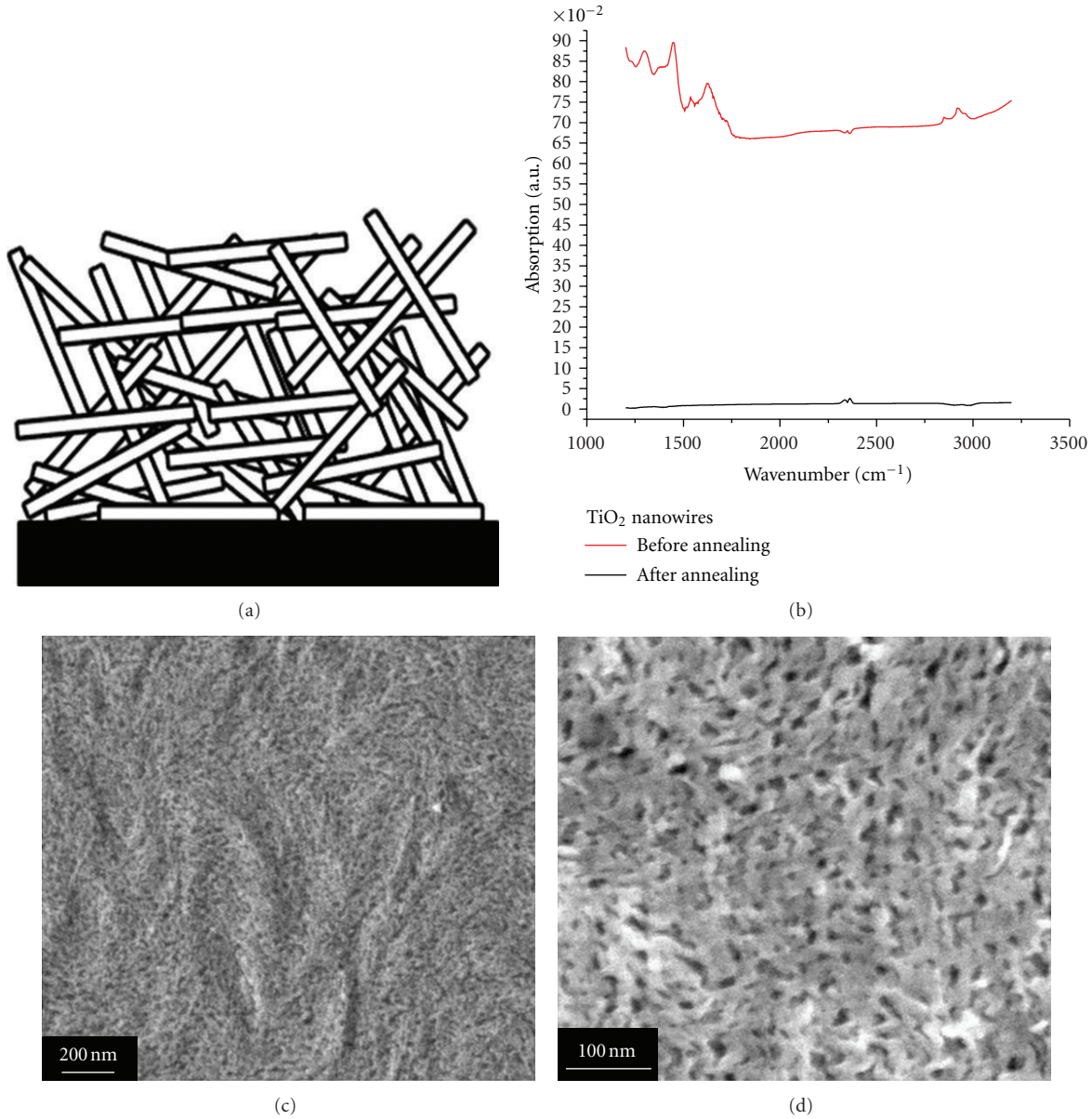

FIGURE 2: (a) A cartoon showing the loosely packed TiO_2 nanowire film fabricated using the dip-coating process. (b) FTIR spectrum of TiO_2 nanowire film dip-coated on a glass slide before and after thermal annealing. (c) SEM image showing the overview of the porous TiO_2 nanostructure. (d) High-resolution second-electron SEM image showing the porous interconnected TiO_2 nanowire network structure after annealing.

on the porous TiO_2 nanowire network film. The strong absorption on the high-energy side combined with the significant quenched and red shifted photoluminescence indicates that efficient electron transfer is achieved between the PbS quantum dots and the porous TiO_2 nanowire. This is also consistent with the superb short-circuit current observed for the porous TiO_2 nanowire-based devices owing to its large interfacial areas and strong electron extraction ability.

4. Conclusions

In summary, we fabricated a high-performance porous TiO_2 film for nanocrystal-sensitized solar cell using an interconnected TiO_2 nanowire network. This facile all-solution-based method simply relies on dip coating and annealing of ultrathin TiO_2 nanowires. This unique nanostructured film provides large interfacial area allowing efficient electron extraction from quantum dots and uses the one-dimensional morphology of the TiO_2 nanowires to favor direct electron transport along the long axial direction to improve electron collection. The heterojunction solar cells using this porous interconnected TiO_2 nanowire network films exhibit a superb J_{sc} of 2.5 mA/cm^2, a large V_{oc} of 0.6 V, and a power conversion efficiency of 5.4% under 8.5 mW/cm^2 white-light illumination. Through the absorption and photoluminescence study of the same PbS quantum dots deposited

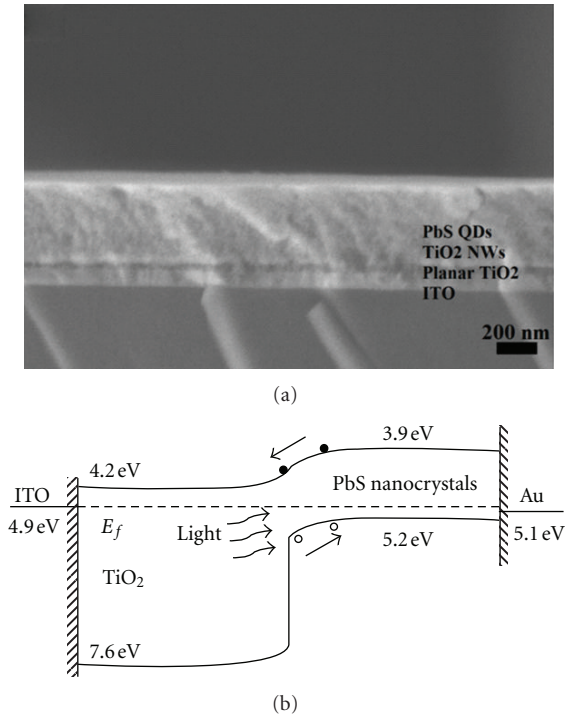

FIGURE 3: (a) SEM image showing the cross-section of the PbS-TiO_2 heterojunction solar cell device. (b) Band diagram of the device.

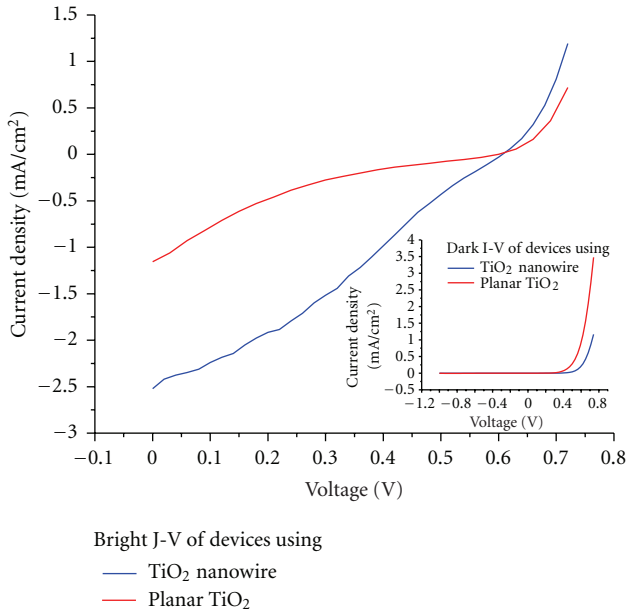

FIGURE 4: Comparison of the current density-voltage (J-V) characteristics under illumination for a standard PbS quantum-dot-sensitized TiO_2 heterojunction solar cell using a planar TiO_2 film formed by conventional sol-gel chemistry with the same solar cell using our thick nanoporous interconnected TiO_2 nanowire network previously deposited on a thin planar TiO_2 film. Both devices are measured under a uniform 8.5 mW/cm^2 white-light illumination. The inset shows the dark I-V characteristics for both devices.

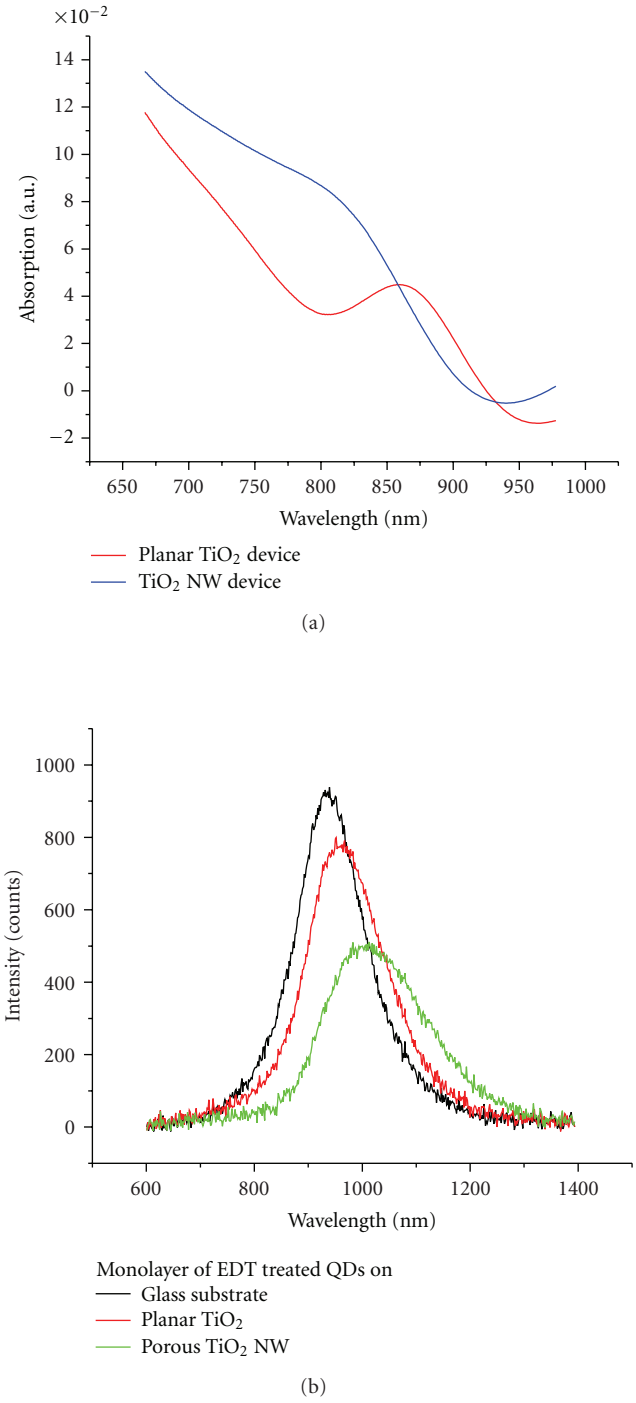

FIGURE 5: (a) Absorption spectrum for the same PbS nanocrystals deposited on planar TiO_2 and porous interconnected TiO_2 nanowire network film. (b) Photoluminescence from a monolayer of the same EDT-treated PbS nanocrystals deposited on glass, on planar TiO_2, on a porous TiO_2 nanowire network film.

on various TiO_2 substrates, we demonstrated a significantly improved electron-transfer efficiency using the TiO_2 nanowire network structure instead of a conventional planar TiO_2 film structure.

Acknowledgments

The authors would like to thank Sangcheol Kim for the absorption measurements and Xiaoqian Ma for FTIR measurements. This work was supported through the AFOSR (FA9550-10-1-0363), through the DARPA COMPASS Program via a Grant from the DOI NBC (N11AP20031), the DARPA young Faculty Award Program and the ETS Institutional Research Chair Program to whom we are most thankful.

References

[1] A. G. Pattantyus-Abraham, I. J. Kramer, A. R. Barkhouse et al., "Depleted-heterojunction colloidal quantum dot solar cells," *ACS Nano*, vol. 4, no. 6, pp. 3374–3380, 2010.

[2] J. M. Luther, J. Gao, M. T. Lloyd, O. E. Semonin, M. C. Beard, and A. J. Nozik, "Stability assessment on a 3% bilayer PbS/ZnO quantum dot heterojunction solar cell," *Advanced Materials*, vol. 22, no. 33, pp. 3704–3707, 2010.

[3] J. J. Choi, Y. F. Lim, M. B. Santiago-Berrios et al., "PbSe Nanocrystal Excitonic Solar Cells," *Nano Letters*, vol. 9, no. 11, pp. 3749–3755, 2009.

[4] T. Ju, R. L. Graham, G. Zhai et al., "High efficiency mesoporous titanium oxide PbS quantum dot solar cells at low temperature," *Applied Physics Letters*, vol. 97, no. 4, Article ID 043106, 2010.

[5] J. M. Luther, M. Law, M. C. Beard et al., "Schottky solar cells based on colloidal nanocrystal films," *Nano Letters*, vol. 8, no. 10, pp. 3488–3492, 2008.

[6] J. Tang, L. Brzozowski, D. A. R. Barkhouse et al., "Quantum dot photovoltaics in the extreme quantum confinement regime: the surface-chemical origins of exceptional air- and light-stability," *ACS Nano*, vol. 4, no. 2, pp. 869–878, 2010.

[7] W. Ma, J. M. Luther, H. Zheng, Y. Wu, and A. P. Alivisatos, "Photovoltaic devices employing ternary PbS_xSe_{1-x} nanocrystals," *Nano Letters*, vol. 9, no. 4, pp. 1699–1703, 2009.

[8] J. Van De Lagemaat, N. G. Park, and A. J. Frank, "Influence of electrical potential distribution, charge transport, and recombination on the photopotential and photocurrent conversion efficiency of dye-sensitized nanocrystalline Tio_2 solar cells: a study by electrical impedance and optical modulation techniques," *Journal of Physical Chemistry B*, vol. 104, no. 9, pp. 2044–2052, 2000.

[9] N. Kopidakis, K. D. Benkstein, J. Van De Lagemaat, and A. J. Frank, "Transport-limited recombination of photocarriers in dye-sensitized nanocrystalline Tio_2 solar cells," *Journal of Physical Chemistry B*, vol. 107, no. 41, pp. 11307–11315, 2003.

[10] B. Liu and E. S. Aydil, "Growth of oriented single-crystalline rutile Tio_2 nanorods on transparent conducting substrates for dye-sensitized solar cells," *Journal of the American Chemical Society*, vol. 131, no. 11, pp. 3985–3990, 2009.

[11] K. Zhu, N. R. Neale, A. Miedaner, and A. J. Frank, "Enhanced charge-collection efficiencies and light scattering in dye-sensitized solar cells using oriented Tio_2 nanotubes arrays," *Nano Letters*, vol. 7, no. 1, pp. 69–74, 2007.

[12] A. Guchgait, A. K. Rath, and A. J. Pal, "Near-IR activity of hybrid solar cells: enhancement of efficiency by dissociating excitons generated in PbS nanoparticels," *Applied Physics Letters*, vol. 9, no. 7, article 073505, 3 pages, 2010.

[13] N. Barati, M. A. F. Sani, H. Ghasemi, Z. Sadeghian, and S. M. M. Mirhoseini, "Preparation of uniform Tio_2 nanostructure film on 316L stainless steel by sol-gel dip coating," *Applied Surface Science*, vol. 255, no. 20, pp. 8328–8333, 2009.

[14] J. Joo, S. G. Kwon, T. Yu et al., "Large-scale synthesis of Tio_2 nanorods via nonhydrolytic sol-gel ester elimination reaction and their application to photocatalytic inactivation of *E. coli*," *Journal of Physical Chemistry B*, vol. 109, no. 32, pp. 15297–15302, 2005.

[15] M. A. Hines and G. D. Scholes, "Colloidal PbS nanocrystals with size-tunable near-infrared emission: observation of post-synthesis self-narrowing of the particle size distribution," *Advanced Materials*, vol. 15, no. 21, pp. 1844–1849, 2003.

[16] J. M. Luther, M. Law, Q. Song, C. L. Perkins, M. C. Beard, and A. J. Nozik, "Structural, optical, and electrical properties of self-assembled films of PbSe nanocrystals treated with 1,2-ethanedithiol," *ACS Nano*, vol. 2, no. 2, pp. 271–280, 2008.

[17] B. Mukherjee, B. Viswanath, and N. Ravishankar, "Functional nanoporous structures by partial sintering of nanorod assemblies," *Journal of Physics D*, vol. 43, no. 45, Article ID 455301, 2010.

[18] B. R. Hyun, Y. W. Zhong, A. C. Bartnik et al., "Electron injection from colloidal PbS quantum dots into titanium dioxide nanoparticles," *ACS Nano*, vol. 2, no. 11, pp. 2206–2212, 2008.

[19] B. -R. Hyun, A. C. Bartnik, L. Sun, T. Hanrath, and F. W. Wise, "Control of electron transfer from lead-salt nanocrystals to TiO_2," *Nano Letters*, vol. 11, no. 5, pp. 2126–2132, 2011.

[20] I. Robel, V. Subramanian, M. Kuno, and P. V. Kamat, "Quantum dot solar cells. Harvesting light energy with CdSe nanocrystals molecularly linked to mesoscopic Tio_2 films," *Journal of the American Chemical Society*, vol. 128, no. 7, pp. 2385–2393, 2006.

[21] W. A. Tisdale, K. J. Williams, B. A. Timp, D. J. Norris, E. S. Aydil, and X. Y. Zhu, "Hot-electron transfer from semiconductor nanocrystals," *Science*, vol. 328, no. 5985, pp. 1543–1547, 2010.